17th World Conference on Earthquake Engineering, 17WCEE
Sendai, Japan - September 13th to 18th 2020

MODELLING OF MASONRY WALL SHEAR STRENGTH AND DEFORMABILITY BY COMBINED FIBER BEAM ELEMENTS

P. Colajanni[(1)], S. Pagnotta[(2)], N. Spinella[(3)].

[(1)] *Associate Professor, Department of Engineering, University of Palermo, Italy, piero.colajanni@unipa.it*
[(2)] *Ph.D. Student, Department of Engineering, University of Palermo, Italy, salvatore.pagnotta@unipa.it*
[(2)] *Researcher, Department of Engineering, University of Messina, Italy, nspinella@unime.it*

Abstract

Seismic assessment of unreinforced masonry (URM) buildings is still a critical issue due to the material and construction technique heterogeneity and complexity. As a matter of fact, several strategies have been developed to model URM behavior, e.g.: equivalent frame, equivalent homogenization, distinct elements. FE 2D and 3D models, with micro- or macro-modelling approach, provide accurate results, though they require a complex calibration and expensive computational efforts. By contrast, 1D models, with lumped or distributed nonlinear behaviour, aim to catch the main structural performance, ignoring local effects. In adapting FE codes developed to model RC frames to the modelling of masonry structures by the equivalent frame approach (EFA), a critical issue is to take into account shear strength and deformability vs axial force variation. In modelling URM buildings by means of EFA, if shear strength dependence on axial force variation is neglected performing nonlinear time-history analyses (NLTHAs) or pushover analyses, the assessment of structural performance could provide inaccurate results. This issue plays a key role, besides the axial force variation induced by the shear strength of the spandrel, especially when vertical seismic action is considered. Indeed, advanced seismic codes (e.g.: ASCE 41-17, NTC 2018) recommend to employ, if necessary, both horizontal and vertical seismic actions during NLTHA, in order to reproduce the earthquake load acting on URM structures during ground motion. In this context, the present paper proposes a new modelling scheme able to reproduce the dependence of the shear strength on the axial force value currently acting on the cross section of the masonry element. The modelling scheme aims to substitute the vertical rigid elements, which are inserted between piers and spandrels in the EFA, with a force-based fiber section element. Its cross section and material properties are calibrated in order to take into account the contribution of both the shear strength and deformability of the masonry pier in the structural analysis. The end sections of the fiber element are constrained aiming at behaving as a shear type element. By using this modelling scheme, reliable results, both in terms of stiffness, strength and post-peak behavior are obtained. Proposed scheme efficiency is proved by favourable comparison against experimental results carried out both on masonry walls and frames.

Keywords: masonry; shear strength and deformability; N-M-V interaction; FEM modeling; equivalent frame.

1. Introduction

The assessment of the seismic vulnerability of masonry buildings is certainly still a challenge for researchers operating in all five continents. In this context, the formulation of mathematical and mechanical models for the "material" masonry and for the numerous morphologies of the masonry structural systems is still one of the problems that has not received completely satisfactory answers. The heterogeneity and complexity of the materials and construction techniques, combined with the influence that the manufacturing methods of the masonry and construction details have on the behaviour of the structure product, making coding of models capable of adequately representing the expected behaviour of the structures in relation to the construction techniques used is extremely complex. As a matter of fact, different strategies have been developed to model behaviour of UnReinforced Masonry structures (URM). Aiming at characterizing the behaviour of the masonry "material", both equivalent homogenization and distinct elements are used, while in capturing the behaviour of the whole structure both micro or macro-modelling approach are followed.

When structures with simple structural morphology are considered, such as in the case of seismic evaluation of single structural unit of residential building, most of the international seismic codes share the idea that calculation approach can diversified if the absence of stiff deck, efficient slab-to-wall, and wall-to-wall connection preclude to ensure a box-like behaviour. Thus, when the masonry wall is not suitably connected to the deck to prevent wall out-of-plane overturning, the seismic response is controlled by out-of-plane failure mechanisms. Simple equations derived by linear and nonlinear kinematic approaches allow one to assess the behaviour under seismic excitation, and they can rule the design of the first effective retrofitting systems to avoid out-of-plane collapse. By contrast, when box-like behaviour of the structure is ensured, a mechanical model able to assess the behaviour of the whole structural unit have to be considered.

To this aim, detailed 2D and 3D Finite Element models with complex constitutive law able to represent the non-linear behaviour of the masonry and its ineffectiveness in tension, and special connection elements able to model the slab-to-wall, and wall-to-wall connections can predict the whole structure seismic behaviour at the cost of large computational efforts. Moreover, in order to obtain adequate level of accuracy, the numerical parameters that characterize the constitutive load of masonry and connection elements should be suitably calibrated, on the basis of in situ or laboratory tests.

In order to cope with the need of practitioners for a simple, easy to manage and to control, still reliable models, macro-modelling approaches was developed since the seventies. Simplified methods able to assess the seismic resistance of a masonry building were formulated after the earthquake of Friuli in 1976; Tomaževič M. [1], and Tomaževič M. and Turnsek, V. [2] developed the POR method, based on the shear resistance of the masonry walls of each story, considered as fixed at the ends. Thus, the behaviour of each storey was assumed to be independent by that of the other storeys. The masonry building seismic resistance was assumed to be coincident with that of the critical story, i.e. the story characterized by the minimum value of the ratio between the horizontal seismic story shear and story shear resistance.

At the end of the last century, aiming at capturing the main structural performances, and ignoring the local effects, Magenes and Della Fontana [3] developed the Equivalent Frame Approach (EFA). Similarly to the modelling of steel or reinforced concrete frames, the masonry building structure model is composed by one dimensional elements, able to represent both the flexural and shear strength and deformability of the piers. The concentrate or distributed non-linear behaviours are modelled by simplified or conventional stress-strain law for the masonry, and/or simplified generalized external force-relative displacements at the ends of the one-dimensional macroelements. Recently, Marques and Lourenço [4] published a state of art report on frame models and macro-element modelling.

Thus, the seismic vulnerability can be evaluated by using the conventional analysis method suggested by seismic codes, i.e. lateral force method or modal response spectrum analysis for linear system, or more advanced static (pushover) or time history non-linear analyses. To this aim, either Finite Element (FE) software codes derived on purpose (e.g., TREMURI by Lagomarsino et al [5], SAM by Magenes and Della Fontana [6] and Magenes et al., [7], 3DMacro by Caliò et al. [8]), or more general FE codes for framed structure (e.g. SeismoStruct by SeismoSoft [9], OPENSEES by Mazzoni et al. [10]).

In adapting the FE codes developed to model RC frames to the modelling of masonry structures using the equivalent frame approach (EFA), a critical problem is that of taking into account the shear strength and deformability with respect to the variation of the axial force.

In modelling URM buildings by means of EFA, if shear strength dependence on axial force variation is neglected performing pushover analyses or Non-linear Time-History Analyses (NLTHAs), the assessment of structural performance could provide inaccurate results. This issue plays a key role, besides the axial force variation induced by the vertical component of seismic action, also in more conventional analysis of equivalent frames due to the masonry piers axial force variation induced to shear strength of the spandrel.

In this context, the present paper proposes a new modelling scheme able to consider the dependence of the shear strength on the axial force value currently acting on the cross section of the masonry element. The modelling scheme aims to substitute the vertical rigid elements, which are inserted between piers and spandrels in the EFA, with a force-based fibre section element. Its cross section and material properties are calibrated in order to take into account the contribution of both the shear strength and deformability of the masonry pier in the structural analysis.

2. The equivalent frame approach

Many different model have been formulated according to the EFA. Among them, the SAM (Simplified Analysis of Masonry Buildings) proposed by Magenes and Della Fontana [7] plays a key role due to its simplicity and being based on solid mechanical model. The model was initially formulated for 2D systems, it was extended to reproduce the behaviour of 3D masonry buildings.

According the EFA, a masonry pier or spandrel is modelled by a deformable part with finite resistance modelled using non-linear beam-column element, and of two infinitely rigid and resistant parts at the ends of the element (Fig. 1) modelling the beam-to-column "nodes", characterized by significant dimensions in equivalent masonry frames.

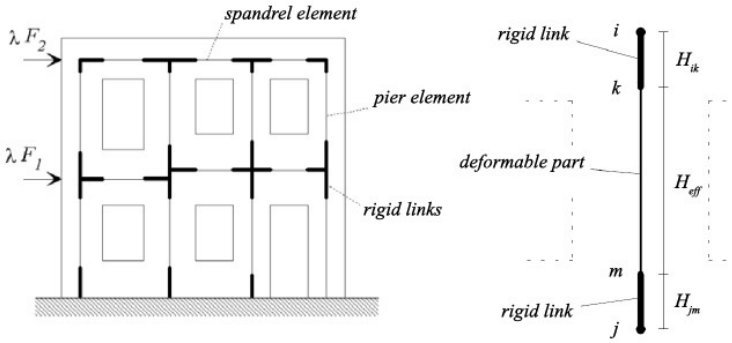

Fig. 1 – Equivalent frame and a pier loaded in the plane schemes.

The height of the deformable part or "effective height" of the pier is defined according to what proposed by Dolce [11], to keep roughly account for the deformability of the masonry in the node areas. More precisely, the effective height H_{eff} of the deformable part of the pier is determined as follows:

$$H_{eff} = h' + \frac{1}{3} D \frac{(H - h')}{h'} \tag{1}$$

where H is the inter-story height, D the width of the masonry pier, and h' is the geometrical height of the pier, determined as depicted in the figure 2 by the intersections of the pier axis with straight line inclined at 30 degrees with respect to the horizontal line, starting from the edge of the door or window. In the original formulation the behaviour of the piers element was assumed to be elasto-plastic with deformation limit. That is, it was assumed that the piers have elastic linear behaviour until one of the possible failure criteria is verified. The stiffness matrix in the elastic phase assumes the usual shape for frame elements with shear

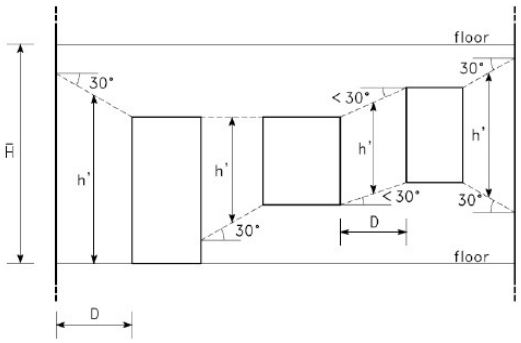

Fig. 2 –Definition of the effective height of the masonry piers.

deformation, and is determined once the Young E modulus, the G modulus are defined, and the geometry of the section.

Many different model for characterizing the behaviour of the pier were developed. Recently, Peruch et al. [12], aiming at reproducing the cyclic behaviour of masonry structure by implementing the equivalent frame model in the open source software OpeenSees [10], used a macroelement consisting in a forced-based beam element joined with a phenomenological shear-relative displacement relationship that describes the shear behaviour derived by mechanical model or experimental test. They stressed that a fibre-section beam-column element allows for a quite accurate modelling of the N-M interaction both in the elastic and non-linear stages, while the force-based formulation, guaranteeing equilibrium between shear and bending moment, ensure a consistent combination between the fibre beam-column element and the phenomenological shear-relative displacement relationship. In order to model the axial stress-strain behaviour in compression of the fibres, they used the "Concrete 02" material of the OpenSees library, that reproduce the simplified Kent and Park constitutive law [13] for the concrete. They also notice that the modelling of material with very low or without tension resistance, as is the main feature of the masonry, can results in convergence difficulty in ensuring local equilibrium. Therefore, they advised to add elastic fibres with negligible area at the corners of the real masonry section, in order to stabilize the convergence procedure, without significantly modified the overall behaviour.

The choice of the phenomenological shear-relative displacement relationship plays a key role in determining the accuracy of the model. Aiming at modelling the cyclic behaviour of the masonry wall, the Authors selected the "hysteretic" uniaxial material of the OpenSees library to reproduce the shear behaviour of the pier, characterized by a trilinear stress-strain relationship. In particular, the Authors described the relationship by means of an elastic branch up to the shear value of V_{el}, the cracked phase up to the achievement of shear capacity V_r, the softening branch up to the attainment of the ultimate shear strength V_u, and finally a constant shear strength residual value. When cyclic behaviour is modelled, the main features of the "hysteretic" material are the capacity of reproducing degraded unloading stiffness based on ductility, pinching of hysteretic cycles during reloading by two parameters that control deformation and force, and two damage parameters linked to ductility and energy demand.

The main parameters that define the shape of the envelope of the trilinear curve are the shear strength V_R and the corresponding strain deformation γ_r. Aiming at modelling the behaviour of existing masonry building, where the failure due to diagonal cracking often precedes the sliding shear failure, the following well know formulation proposed by Turnšek and Čačovič [14] is assumed:

$$V_r = \frac{f_{mt}\, l\, t}{b}\sqrt{1-\frac{N}{f_{mt} l\, t}} \tag{2}$$

being f_{mt} = the diagonal tensile resistance of the masonry, l and t the dimensions of the resisting pier section, b a coefficient related to the pier slenderness H/l and N the axial stress acting on the section. The minus sign in the second-member radical in Eq. (2), instead of the more common positive sign, arises from having

assumed N positive if traction. The value of the shear at the end of the elastic branch V_{el} = 0.6 V_r was assumed, and the corresponding shear deformation γ_{el} given by the following relation

$$\gamma_{el} = c_{el} \frac{\chi V_{el}}{G_m l t} \tag{3}$$

being k the shear coefficient (χ = 1.2 for rectangular section), G_m the shear modulus of the masonry, and c_{el} a suitably coefficient derived by experimental test. Shear deformation γ_R at the attainment of the shear strength, and the ultimate shear V_u and deformation γ_u can be derived either by matching experimental results, seismic code indication, or theoretical model.

Lastly, the Authors stressed that the equivalent element implemented in the OpenSees software in [12] and in previous papers [15] are not able to represent the variation of the shear resistance with variation on axial load N, since the features of the elements derived for reinforced concrete frame do not easily allows the modelling of such a behaviour.

In the following section, it will be shown as a simple substitution of the rigid element placed at the end of piers and spandrels with a force-based beam-column element with equivalent suitably calibrated fibre section dimensions and trilinear stress-strain law is able to model shear strength and deformation taking into account the effect of the variation of the axial force.

3. Equivalent force-based element for shear strength and deformation modelling

When using calculation software designed for the analysis of reinforced concrete or steel framed systems for the simulation of the behaviour of masonry structures through the equivalent frame approach, one of the most important problems is the modelling of the dependence of the shear strength on the actual value of the axial force. While for reinforced concrete element, sophisticated model able to capture interaction between axial/flexural and shear behaviour of RC structural walls and columns under cyclic loading are available [16], shear strength of masonry element is often still modelled neglecting its dependence on axial force. This assumption makes not possible of taking into account the changes in shear strength during seismic events in which the vertical component of the seismic acceleration has significant effects. Moreover, it does not even allow to model the changes in the pier shear strength in simple pushover analyses, where the effect of the frame behaviour ensured by the spandrel of significant strength it induces appreciable variations of the normal stress in the piers.

This drawback cannot be immediately resolved into the common beam elements implemented in any FE software that models the non-linear behaviour of one-dimensional beam elements, because shear strength is not usually coupled with axial force.

Nonetheless, the equilibrium equations of the element in the absence of loads orthogonal to the axis can be written in the following form:

$$V = \left(1 + \alpha_i\right) M_j \big/ H \tag{4}$$

where M_j is the bending moment at the base of the element, and $\alpha_i = M_i/M_j$ the ratio of the bending moment at the ends i and j of the element. Commonly is not possible to link the shear force to the value of the bending moment at one end of the element, since the shape of the bending moment diagram, i.e. the value of α_i is not known a priori. In clamped-free element, or in clamped-clamped element (Grinter type), trivial relations between bending moment end and shear force is known, namely $V=M_j/H$ (α_i = 0) and V = 2 M_j/H (α_i = 1) respectively. However, it is noteworthy that in elements that are symmetrical with respect to the midpoint without lateral loads applied along the element axis, when the end rotations are equal, α_i = 1.

On these bases, the proposed model substituted at the rigid links at the end of the pier one beam-column deformable element, that in the following will be denoted as Equivalent Shear Strength Element (ESSE). At the ESSE end sections a constrain that imposes equal end rotations is assigned, in order to have a

simple unique law linking the shear V and end moments M_{sr} value (Fig. 3), namely $M_{sr} = V\,H_{sr}\,/2$ ($sr = ik, mj$), where H_{sr} is the length of the ESSE. If the pier shear deformability is not included in the flexible part of the model, the ESSE will be characterized by a flexural deformability equal to half (or one) of the shear deformability of the actual piers, otherwise negligible deformability will be assigned at the element. Moreover, the element is composed by a beam with hinges element with an elastic interior element. The end section dimensions and fibre axial stress-strain law suitably defined, so as the bending moment-plastic hinge rotation relationship are able to reproduce, via the relation $M_{sr} = V\,H_{sr}\,/2$, the phenomenological shear-relative displacement relationship assumed for characterizing the shear behaviour of the pier, taking into account the shear strength dependence on axial force value. This is obtained by initially governing the strength of the element, then suitably adapting the deformability.

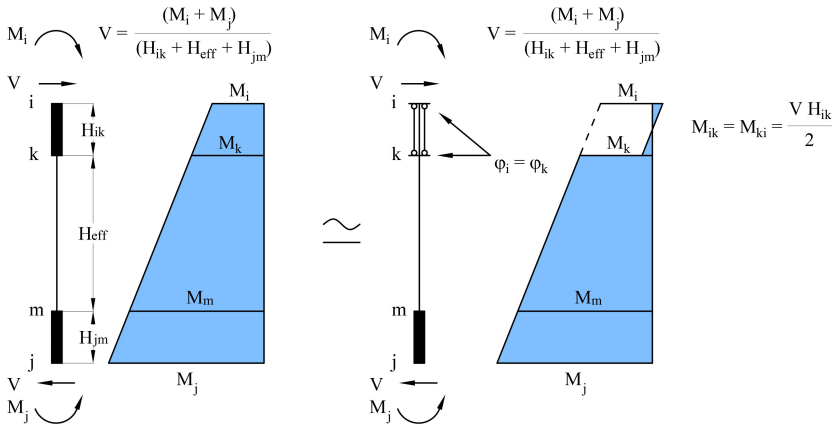

Fig. 3 – Bending moment distribution along the pier in conventional and proposed (ESSE) model

3.1 Modelling of the shear resistance

In order the ESSE be able to reproduce the phenomenological shear-relative displacement relationship assumed for characterizing the shear behaviour of the pier, a bending moment-flexural curvature relationship that resemble the shape of stress-strain deformation of the fibre will be designed. To this aim, an ideal section formed by only two fibre of area A_f placed at distance $d/2$ by the element axis is assigned to the 2D ESSE. Aiming at ensuring that at the end of the elastic branch of the moment-curvature relationship, the shear force is equal to V_{el}, a linear first branch of the fibre stress-strain law with the same Young modulus in tension and compression is assumed. Thus, the section fibre stress can be expressed as a function of external axial load N and bending moment M_{ik} as follows:

$$\sigma = \frac{N}{2\,A_f} \pm \frac{M_{ik}}{A_f\,d} \tag{5}$$

In order to reproduce the variation of the shear strength with axial force variation expressed by Eq. (2) in the expected range of variation of the axial load [$N_{min} \le N_v \le N_{max}$] around the value N_v induced by the gravity loads, Eq. (2) is linearized in the form:

$$V_R(N) = V_0 - \beta N \tag{6}$$

where the slope β and V_0 can be evaluated by the least squares method in the axial force variation range where either the external axial force is expected or a shear failure rather than a flexural one is expected [$N_{min} \le N \le N_{max}$]. Alternatively, the V_0 value can be fixed in order to ensure that, for the axial load given by gravity load N_v Eq. (6) provide the "actual" pier shear strength V_v, i.e. evaluated assuming $N = N_v$ in Eq. (2).

Aiming at modelling the shear strength of the piers through the ESSE, an arbitrary value can be assigned to the equivalent limit stress in tension $f_{r,t}$ of its fibres. The dimensions of the section fibre A_f that ensures that, when the shear force attains the value V_R, the most tension fibre reaches $f_{r,t}$ will be derived on

this $f_{r,t}$ value, and on the basis of the Eq. (5) and Eq. (6). More precisely, taking into account that in the ESSE the end sections are constrained to have the same rotation, and thus $V = 2\ M_{ik}/H_{ik}$ according to Fig.1, when the latter relation is substituted in Eq. (5), the following relation is obtained:

$$\sigma = \frac{N}{2\,A_f} \pm \frac{V H_{ik}}{2 A_f\, d} \tag{7}$$

By imposing that, when the shear force in Eq. (7) attains the limit value given by Eq. (6), the maximum tension stress in Eq. (7), obtained by assuming the positive sign in the second term of right hand side, reaches the limit value $f_{r,t}$ one obtains:

$$\frac{2 A_f d}{H_{ik}} f_{r,t} - \frac{N\,d}{H_{ik}} = V_0 - c\,N \tag{8}$$

For the principle of identity of polynomials, the dimensions of the equivalent section can be evaluated as follows:

$$d = c\,H_{ik};\ A_f = \frac{V_0\,H_{ik}}{2\,d\,f_{r,t}} \tag{9a,b}$$

Once the dimensions of the equivalent section able to guarantee the dependence of the shear resistance on the axial force required by the Turnšek and Čačovič relationship was determined, a fictitious elastic modulus E_{fic} was defined, so as to ensure that the ESSE reproduced the elastic (first branch) shear deformability of the actual pier. Taking into account that the flexural stiffness $K_{el,ik}$ of the ESSE with the constrain at the end rotation can be evaluated as that of an elastic shear type element (Grinter deformation), the equivalent elastic stiffness can be evaluated equating it to the pier elastic shear deformability provided by Eq. (3) for $V_{el} = 1$. Thus, the following relation is derived:

$$\frac{1}{K_{ik,el}} = \frac{H_{ik}^3}{12\,E_{fic}\left(2\,A_f\,d^2/4\right)} = c_{el}\,\frac{k\,H_{eff}}{G_m\,l\,t} \tag{10}$$

If the model of the flexible part of the pier does not include the shear deformation, the value of E_{fic} of the ESSE fibre first branch of the stress-strain law can be evaluated from Eq. (8). Otherwise, a value 100 times greater than the former can be assumed, in order to ensure that the increased deformability introduced by substituting the rigid offset with the ESSE does not exceed 1% of the pier shear deformability.

3.2 Modelling of the phenomenological shear-displacement relationship

In order to ensure that ESSE is able to reproduce the phenomenological shear-displacement relation of the piers depicted in Fig.4a), it has to be ensured that in the ESSE when the shear attains the maximum strength, the relative displacement due to the shear attains the value $\delta_r^v = \gamma_r\,H_{eff}$. To this aims, it is noteworthy that, once the section is constituted by two fibres only, only equilibrium equations provide the stress in each of the two fibre. Thus Eqq. (7-9) holds at each stage, irrespective of the shape of the stress-strain law. This means that, once the area of each fibre A_f is determined, for any given value of the shear V_x, (x = *el, r, u*) the corresponding stress in the tensile fibre f_{tx} can be evaluated by the rotational equilibrium equation of the equivalent section with respect to the compressed fibre:

$$f_{tx} = \frac{1}{2A_f}\left(V_x\,\frac{H_{ik}}{d} + N\right) \quad (x = el, r, u, \ldots.) \tag{11}$$

In Eq. (11) $N = N_v$ is assumed for fibre stress-strain law calibration, taking into account that the phenomenological shear-displacement relation in Fig.4a is provided for $N = N_v$. The stress in the compressed fibre f_{cx} is computed by substitution in Eq. (11) of V_x with $-V_x$, i.e. $f_{cx} = (-V_x\,H_{ik}/d + N)$.

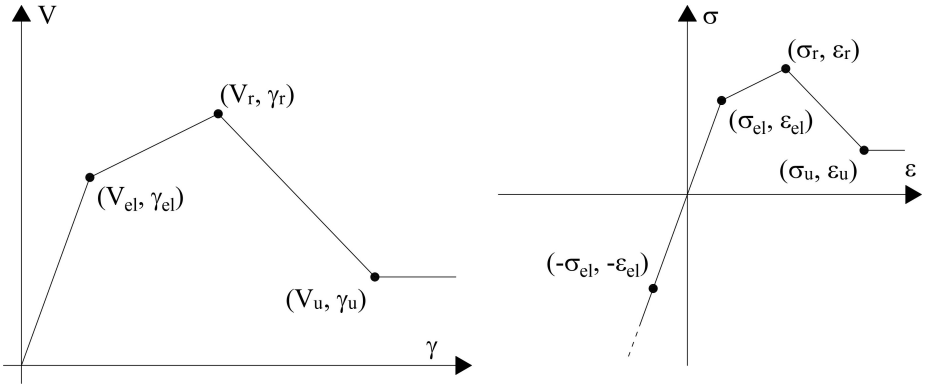

Fig. 4 – a) Phenomenological shear-deformation of the pier; b) stress-strain relationship of the fibre of ESSE end sections

Now, the fibre stress-strain law is defined in order to ensure that the actual pier and the one with the ESSE have the same shear deformability in each branch of the curve. The ESSE non-linear behaviour will be modelled by the plastic hinge at the ends of the element in which the one-point Endpoint Hinge Integration procedure [17] is selected. It is characterized by integration points placed at the element ends. Once an arbitrary (e.g. $H_{ik}/100$) value of the plastic hinge length l_p is selected, the end relative displacement $\delta_{ik,r}$ at the attainment of the V_r shear is given by the following relation:

$$\delta_{ik,r} = \delta_{ik,el} + \left(\phi_r - \phi_{el}\right) l_p \left(H_{ik} - \frac{l_p}{2}\right) \tag{12}$$

where $\delta_{ik,el} = V_{el}/K_{ik,el} = \gamma_{el} H_{eff}$ is the elastic relative displacement due to the shear deformation, and $\phi_{el} = (V_{el} H_{ik}/2)/(E_{fic} A_f d^2/4)$ and ϕ_r are the end section curvature at the attainment of the elastic $\delta_{ik,el,}$ and $\delta_{ik,r} = \gamma_r H_{eff}$ relative displacement respectively. Thus, the value of ϕ_r can be easily evaluated by Eq. (12). In order to easily control the values of the fibre axial strain at each curvature stage, the stress-strain law in compression is set as elastic with Young modulus E_{fic} (Fig. 4b). Thus, the axial strain of the compressed ε_{cr} and tensile fibre $\varepsilon_{tr} = \varepsilon_r$ at the r stage can be easily evaluated as follows:

$$\varepsilon_{cr} = f_{cr} / E_{fic}; \qquad \varepsilon_{tr} = \varepsilon_r = \phi_r d + \varepsilon_{cr} \tag{13}$$

The equality $\varepsilon_{tr} = \varepsilon_r$ stresses that Eq. (13) provide the characteristic value that have to be assigned at the fibre stress-strain law in tension. Once the maximum shear strength is reached, a constant or a softening branch characterizes the phenomenological shear-displacement law. In order to ensure that the ESSE element does not lose the ability to carry the gravity load, while the shear strength is reducing, the fibre stress-strain law in compression is characterized by in infinitely ascending branch with the same young modulus of the previous branch. By contrast, the tension branch which will determine the shape of the moment-curvature law of the section, will be determined by a procedure similar at the previously described one. More precisely, denoting with $\delta_{ik,u}$ the relative displacement due to the attainment of the ultimate shear deformation γ_u in the actual pier, with ε_{cu} and $\varepsilon_{tu} = \varepsilon_u$ the corresponding compressed and tension fibre strain respectively, and ϕ_u the corresponding curvature value in the end sections of the ESSE, their values can be derived as follows:

$$\delta_{ik,u} = \delta_{ik,r} + \left(\phi_u - \phi_r\right) l_{p,ik} \left(H_{ik} - \frac{1}{2} l_{p,ik}\right) \tag{14}$$

$$\varepsilon_{cu} = f_{cu} / E_{fic}; \qquad \varepsilon_{tu} = \varepsilon_u = \phi_u d + \varepsilon_{cu} \tag{15a,b}$$

Once all the geometrical and mechanical characteristics of the ESSE were defined, in the next sections validation of the proposed model will be carried out.

4. Model validation

4.1 Validation against experimental results

A first validation of the model is performed by showing that the model is able to reproduce with a great accuracy the results of an experimental test with a prefixed values of the axial load. Moreover, it will be shown which is the assessment of the response provided by the model when the axial load is changed.

The test was carried out by Abrams and Shah [18], and was used in [12] and [15] for model validation. The analysed pier has cross section dimensions $l = 2.743$ m and $t = 0.198$ m, height $H = 1.626$ m, and masonry compression and shear strength $f_m = 6.28$ MPa and $f_{tm} = 0.15$ MPa respectively. The elasticity and shear moduli are $E_m = 2460$ MPa and $G_m = 1130$ MPa. The pier was loaded with a low axial force of $N_v = 282$ kN, corresponding to a normalized axial load $n = N_v/(f_m\ l\ t) = 0.083$. In Fig. 5a) the shear-displacement experimental curve is reported, together with its piecewise approximation, characterized by the following point: (V_{el}=146.3 kN; δ_{el}=1.143 mm) - (V_r=180.5 kN; δ_r=5.0 mm) - (V_u=121.5 kN; δ_r=12.807 mm). Since Eq. (2) evaluated for $N=N_v$ assesses a shear strength of 172 kN, Eq. (2) and Eq. (6) will be multiplied by a factor α_r = 180.5/172.0=1.048 in order to have the predicted shear strength coincident with the experimental one. In Fig.5b) the shear strength domain due to flexural and shear failure, i.e. $V_{flex} = M_w/H = N\ l/(2\ H)[1-N/(t\ l\ f_m)]$ and Eq. (2) are compared. Assuming as range of linearization of Eq. (2) the N value for which a shear failure occurs, namely 184.5 kN ≤ N ≤ 2697.5 kN, and enforcing that for the actual axial load the linearized curve provides the actual shear strength of the pier, the slope $\alpha_r\ c = 0.13$ and $\alpha_r\ V_0 = 141.79$ kN are found. The obtained linearized shear strength is also depicted in Fig.5b) as $\alpha_r\ V_{rl}$.

Denoting with I_m the pier inertia modulus, $\delta_x^f = V_x\ H^3/(3\ E_m\ I_m)$, and δ_x^v the flexural and shear rate of the masonry pier displacement at the x state (x = el, r, u), δ_x^v can be evaluated as follows $\delta_x^v = \delta_r - \delta_x^f$, obtaining δ_{el}^v = 0.893 mm, m, δ_r^v = 4.69 mm, δ_u^v = 12.6 mm. Since no rigid element has to be considered in the equivalent frame approach, the height of the ESSE element H_{ik} was set equal to 0.01 m in order not to significantly modify the pier flexural deformability, and a plastic hinge end section lengths $l_p = 0.1$ mm is arbitrarily chosen. If the arbitrary value of $f_{r,t} = 0.15$ MPa is selected, Eq. (9a) and Eq. (9b) provide A_f = 3.446 m^2 and Eq. (10) $E_{fic} = 4.211$ Mpa. It is noteworthy that all the above and the following parameters of the ESSE are not intended to characterize a mechanical model, but a "mathematically" equivalent model, and therefore they can take on values devoid of any physical meaning. Eq. (11) particularized at the elastic limit el provides the value of fibre strength $\varepsilon_{el} = 2.7\%$, and corresponding stress $f_{el,t} = E_{fic}\ \varepsilon_{el} = 0.113$ Mpa, and the correspondent value of the ESSE end section curvature can be evaluated as $\phi_{el} = (V_{el}\ H_{ik}/2)/(E_{fic}\ A_f\ d^2/4)$ = 53.59 m^{-1}. At the attainment of the pier shear strength V_r, once the equality of the displacement due to shear deformation of the actual pier δ_r^v and that of the ESSE element $\delta_{ik,r}$ is enforced, the value of the plastic hinge curvatures of the ESSE element at the r stage is evaluated by Eq. (12), obtaining ϕ_r = 3667 m^{-1}. The corresponding value of the compressed fibre stress is evaluated as $f_{cu} = (-V_x\ H_{ik}/d + N) = 0.231$ MPa, and Eq. (13b) provides the value of the fibre strain at the attainment of element shear strength $\varepsilon_r = 4.97$. Then, the relative displacement of the ESSE element at the ultimate state $\delta_{ik,u}$ is set equal to the shear rate of the ultimate displacement at the ultimate state of the actual pier δ_u^v. Thus by means of Eq. (14) the ultimate curvature of the ESSE end section ϕ_u = 11991 m^{-1} is calculated. Finally, since in the compressed fibre f_{cu} = 0.169 MPa, Eq. (15b) provides ε_{tu} = 16.4.

In Fig. 5a) the numerical FEM base shear vs. top displacement curve is reported, showing that it is almost coincident with the target curve. In Fig.5b) the shear strength obtained by the numerical analysis performed with the same model and different axial load is compared with the theoretical shear strength, proving the efficiency of the model to capture the chosen shear strength vs. axial load variation. Lastly in Fig. 5c) the shear-drift response obtained for the different axial load value is reported, showing that the model predicts a reasonable V_{el} and V_u vs. axial load variation, the former due to the delay in the cracking stage, the latter due to the increasing in the effect of the friction. Lastly, it has to be remarked that in this example, the largest variation of the axial force was modelled. For smaller range of variation, a more precise control of these last two shear characteristic values, namely V_{el} and V_u, can be accomplished.

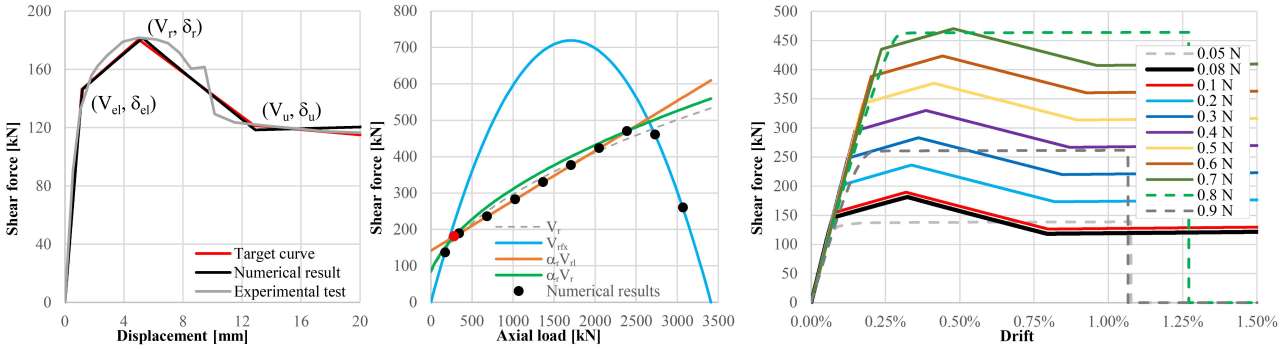

a) b) c)

Fig. 5 – a) Abrams and Shah [18] panel: a) V–δ base shear displacement curves; b) shear –axial force interaction domain; c) FEM response for different axial load

4.2 Phenomenological shear-displacement relationship suggested by seismic codes.

Secondly, the ability of the model in reproducing the shear strength versus axial force variation is shown by checking its ability of reproducing the shear-displacement relationship suggested by the Italian seismic code [19] for a clamped-free isolated masonry pier. The shear-displacement relationship is characterized by an elastic perfectly plastic behaviour, with flexural strength evaluated as $M_{fu} = N\,l\,/\,2\,[1\text{-}N\,/\,(t\,l\,f_m)]$ and shear strength, provided by Eq. (2), and the flat plastic branch has an ultimate displacement for flexural failure equal to $\delta_{uf} = 1\%\ H$ and for shear failure $\delta_{uv} = 0.5\%\ H$. Once the ultimate displacement is reached, the piers loses the ability to carry horizontal force, while axial load can be carried out until the whole structure failure.

The analysed pier has cross section dimensions $l = 3.0$m and $t = 0.6$ m, height $H = 1$ m, and masonry design compression normal strength $f_m = 1$ MPa, and elasticity and shear moduli $E_m = 870$ MPa and G_m=362.5 MPa was selected. To show the level of reliability of the proposed element, the entire range of variation of the axial force N has been considered, namely $0 \le N \le N_{max} = l\,t\,f_m = 1800$ kN. A diagonal shear strength V_r provided by Eq. (2), and a flexural shear strength $V_{r,fx} = M_r / H$ was assumed. Assuming an axial load given by gravity load $N_v = N_{max} / 2 = 900$ kN, the shear-relative displacement relationship that have to be simulated with the ESSE element is characterized by a straight elastic branch up to the shear strength $V_r = 440.9$ kN. Denoting with δ_r^f and δ_r^v the flexural and shear rate of the masonry pier displacement at the attainment of the shear strength V_r, the corresponding total displacement is $\delta_r = \delta_r^f + \delta_r^v = V_r\,H^3/(3\,E_m\,I_m) + V_r\,c_{el\chi}\,\chi\,H/(\,l\,t) = 1.25\text{x}10^{-4}\text{m} + 1.621\text{x}10^{-3}\text{ m} = 1.747\text{x}10^{-3}\text{m}$, where I_m is the pier inertia modulus. At the ultimate state, the total displacement for shear or flexural failure are $\delta_u^v = 0.5\%\,H = 5\text{x}10^{-3}$ m., or $\delta_u^f = 1\%\,H = 1\text{x}10^{-2}$ m, respectively, while the flexural component remains unchanged, i.e. $\delta_u^f = \delta_r^f$, since $V_u = V_r$.

Assuming as a centroid of the range of linearization of Eq. (2) N_v, the parameters for the linearized form in Eq. (6) are $V_0 = 233.0$ kN and $c = 0.225$. Since no rigid element have to be considered in the equivalent frame approach, the height of the ESSE element H_{ik} was set equal to H/100 = 0.01 m in order not to modify the pier flexural deformability. If the arbitrary values of $f_{r,t} = 0.1$ MPa is selected, Eq. (9a) and Eq. (9b) provide $A_f = 5.166$ m^2 and Eq. (10) $E_{fic} = 1.724$ MPa. Since a linear behaviour until reaching of the shear strength V_r has to be modelled, i.e. $V_{el} = V_r$, the following values are selected: $\varepsilon_r = \varepsilon_{el} = f_{r,t} / E_{fic} = 0.580$ and $f_{e,t} = f_{r,t}$. In order to achieve an elastic-perfectly plastic behaviour ($V_u = V_r$) until the target displacement capacity for shear failure $\delta_{uv} = 0.5\%\,H = 5\text{x}10^{-3}$ m, $f_{u,t} = f_{r,t}$ is also selected. Since $V_u = V_r$ the flexural rate of the ultimate displacement δ_u^f is equal to δ_r^f. Thus, the predicted value of the shear displacement at the ultimate condition is $\delta_r^v = \delta_{uv} - \delta_u^f = 5\text{x}10^{-3}$ m $- 1.25\text{x}10^{-4}$m $= 4.87\text{x}10^{-3}$m. In order to evaluate the fibre strain at the ultimate condition according to Eq. (14) and Eq. (15), the curvature at the $r = el$ stage is evaluated as $\phi_r = \phi_{el} = (V_r\,H_{ik}/2)/(E_{fic}\,A_f\,d^2/4) = 96.22$ m^{-1}. Then, a,b) the relative displacement of the ESSE element at the ultimate state $\delta_{ik,u}$ is set equal to the shear rate of the ultimate displacement at the ultimate state of the actual

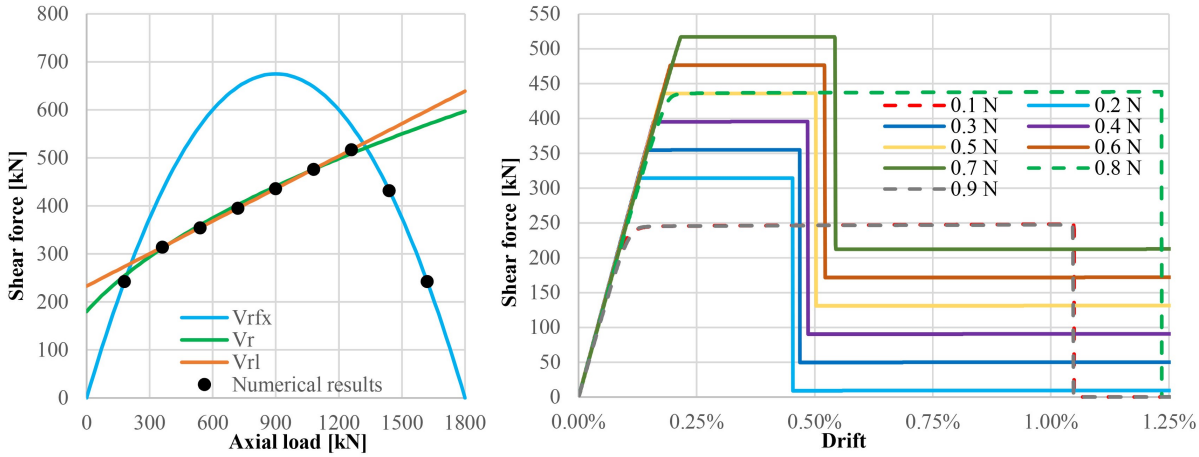

Fig. 6 –Panel that simulate code prescription: a) shear –axial force interaction domain; b) FEM response for different axial load

pier δ_u^v, the latter obtained as the difference of the whole displacement due to shear failure δ_{uv} and the flexural rate δ_u^f, i.e. $\delta_{ik,u} = \delta_u^v = \delta_{uv} - \delta_u^f = 5\text{x}10^{-3}$ m-$1.25\text{x}10^{-4}$m =$4.875\ \text{x}10^{-3}$m. Thus by means of Eq. (14) the ultimate curvature of the ESSE end section $\phi_u = 3371\ \text{m}^{-1}$ is calculated; finally, since in the compressed fibre $\varepsilon_{cu} = \varepsilon_{cr} = f_{tr,}$ Eq.(15b) provides $\varepsilon_{tu} = 7.44$. Lastly, since once the ultimate condition is reached, the pier shear strength has to drop to a small value, a residual value of the fibre stress ε_{tres} can be evaluated (for a fixed axial force N) from Eq. (11). In the following numerical example, the value ε_{tres} was set in order to fix a vanishing residual shear strength for $N_v = 0.3\ N_{max}$=540 kN.

In Fig.6 a) the shear-axial force interaction domain for flexure V_{rfx} and shear V_r failure is compared, and the linearized form of the latter V_{rl} is also reported. The dots represent the values of the shear strength obtained by the FEM, confirming the ability of the ESSE model to reproduce the pier shear strength vs. axial load variation with great accuracy. In Fig.6b) the force-displacement relationship proves that the calibration of the fibre stress-strain law is able to reproduce the prefixed deformation capacity with great accuracy for the prefixed axial load $N = N_v = 0.5\ N_{max.}$ For other axial load values, a variation of the ultimate displacement and the residual shear strength is obtained, both of them accurately estimated by the analytical model. Lastly, it has to be remarked that, in order to tune the flexural displacement capacity of the deformable part of the model of the pier, the ultimate deformation of the stress-strain law of the fibre of the section of the masonry pier can be tuned by evaluating the ultimate curvature of the plastic hinge $\phi_{m,u}$ by adapting Eq. (14) at the flexural deformation of the piers, and evaluating the ultimate strain ε_{mu} that has to be assigned at the masonry stress-strain law as follows:

$$\varepsilon_{mu} = f_m / E_m + \left(\phi_{m,u} - \phi_{m,el}\right)\frac{N}{f_m\, t} \tag{16}$$

where $\phi_{m,el}$ is the curvature of the base section of the piers at the attainment of the masonry strength f_m.

5. Conclusion

A new FEM element was derived, able to reproduce the shear strength vs. axial force variation of masonry element. The modelling scheme aims to substitute the vertical rigid elements, which are inserted between piers and spandrels in the equivalent frame approach, with a force-based fibre section element. Its cross section and material properties are calibrated in order to take into account the contribution of both the shear strength and deformability of the masonry pier in the structural analysis. The end sections of the fibre element are constrained aiming at behaving as a shear type element. By using this modelling scheme, reliable results, both in terms of stiffness, strength and post-peak behaviour are obtained. Proposed scheme efficiency

was proved by favourable comparison against both experimental results carried out on masonry piers and phenomenological shear-displacement relationship suggested by seismic codes.

6. References

[1] Tomaževič M. (1978). The Computer Program POR. Report ZRMK, Ljubljana, [in Slovenian].

[2] Tomaževič M. and Turnsek, V. (1982). Verification of the seismic resistance of masonry building *Proc. of the British Ceramic Society*, 30. 360-369, Shelton House, Stoke on Trent

[3] Magenes G, and Della Fontana A (1998). "Simplified non-linear seismic analysis of masonry buildings". *Proc. of the British Masonry Society*, 8. 190-195

[4] Marques R, Lourenço PB. (2011) Possibilities and comparison of structural component models for the seismic assessment of modern unrein-forced masonry buildings. *Comput Struct*. 89 (21-22):2079-2091

[5] Lagomarsino S, Penna A, Galasco A, Cattari S. (2013) TREMURI program: an equivalent frame model for the nonlinear seismic analysis of masonry buildings. *Eng Struct* .;56:1787 -1799.

[6] Magenes G, Della Fontana AD (1998). Simplified nonlinear seismic analysis of masonry buildings. *Proc Br Masonry Soc*. 8:190-195.

[7] Magenes, G., Remino, M., Manzini, C., Morandi, P., Bolognini, D., (2006) "SAM II, Software for the Simplified Seismic Analysis of Masonry buildings", University of Pavia and EUCENTRE.

[8] Caliò I, Marletta M, Pantò B. (2012) A new discrete element model for the evaluation of the seismic behaviour of unreinforced masonry buildings. *Eng Struct.*;40:327-338

[9] SeismoSoft. SeismoStruct – a computer program for static and dynamic nonlinear analysis of frames structures, 2020. Available at http://www.seismosoft.com

[10] Mazzoni S, McKenna F, Fenves GL (2005). OpenSees command language manual. *Pacific Earthquake Engineering Research (PEER) Center*.

[11] Dolce M (1991): Schematizzazione e modellazione degli edifici in muratura soggetti ad azioni sismiche, L'Industria delle Costruzioni, 25, 44-57 [in Italian].

[12] Peruch M, Spacone E, Camata G (2019): Non linear analysis of masonry structure using fiber-section line elements, *Earthquake Engineering & Structural Dynamics*, 1-20, DOI: 10.1002/eqe.3188

[13] Kent DC, Park R. (1971):Flexural members with confined concrete. *J Struct Div*.; 97(7):1969-1990.

[14] Turnšek V, Čačovič F. (1970): Some experimental results on the strength of brick masonry walls. *Proceedings of the 2nd International Brick & Block Masonry Conference*, Stoke-on-Trent, 1970; 149–156.

[15] Raka E, Spacone E, Sepe V, and Camata G (2015): Advanced frame element for seismic analysis of masonry structures: model formulation and validation, *Earthquake Engineering & Structural Dynamics*, 44, 2489-2506, DOI: 10.1002/eqe.2594

[16] Kolozvari K., Orakcal K., and Wallace J. W. (2015). "Modeling of Cyclic Shear-Flexure Interaction in Reinforced Concrete Structural Walls. I: Theory", *ASCE Journal of Structural Engineering*, 141(5).

[17] Scott M.H. (2011) Numerical integration options for the force-based beam-column element in OpenSees, Oregon State University, Corvallis, available at http://opensees.berkeley.edu /wiki/images/a/ab /IntegrationTypes.pdf.

[18] Abrams DP, Shah N. (1992) Cyclic load testing of unreinforced masonry walls. *Report No. 92-26-10, Advanced Construction Technology Center*—University of Illinois: Urbana, 1992.

[19] D.M. LL. PP. Norme Tecniche per le Costruzioni (Construction Technical Codes). Gazzetta Ufficiale; 20 Feb 2018 (in Italian)

